JOURNAL OF VIROLOGY, Dec. 1998, p. 9645–9655 Vol. 72, No. 12
0022-538X/98/$04.00+0

Effect of Bafilomycin A1 and Nocodazole on Endocytic Transport in HeLa Cells: Implications for Viral Uncoating and Infection

NORA BAYER,[1] DANIELA SCHOBER,[1] ELISABETH PRCHLA,[1] ROBERT F. MURPHY,[2] DIETER BLAAS,[3] AND RENATE FUCHS[1]*

Department of General and Experimental Pathology[1] and Institute for Biochemistry,[3] University of Vienna, Vienna, Austria, and Department of Biological Sciences, Carnegie Mellon University, Pittsburgh, Pennsylvania 15213[2]

Received 1 June 1998/Accepted 9 September 1998

Bafilomycin A1 (baf), a specific inhibitor of vacuolar proton ATPases, is commonly employed to demonstrate the requirement of low endosomal pH for viral uncoating. However, in certain cell types baf also affects the transport of endocytosed material from early to late endocytic compartments. To characterize the endocytic route in HeLa cells that are frequently used to study early events in viral infection, we used ^{35}S-labeled human rhinovirus serotype 2 (HRV2) together with various fluid-phase markers. These virions are taken up via receptor-mediated endocytosis and undergo a conformational change to C-antigenic particles at a pH of <5.6, resulting in release of the genomic RNA and ultimately in infection (E. Prchla, E. Kuechler, D. Blaas, and R. Fuchs, J. Virol. 68:3713–3723, 1994). As revealed by fluorescence microscopy and subcellular fractionation of microsomes by free-flow electrophoresis (FFE), baf arrests the transport of all markers in early endosomes. In contrast, the microtubule-disrupting agent nocodazole was found to inhibit transport by accumulating marker in endosomal carrier vesicles (ECV), a compartment intermediate between early and late endosomes. Accordingly, lysosomal degradation of HRV2 was suppressed, whereas its conformational change and infectivity remained unaffected by this drug. Analysis of the subcellular distribution of HRV2 and fluid-phase markers in the presence of nocodazole by FFE revealed no difference from the control incubation in the absence of nocodazole. ECV and late endosomes thus have identical electrophoretic mobilities, and intraluminal pHs of <5.6 and allow uncoating of HRV2. As bafilomycin not only dissipates the low endosomal pH but also blocks transport from early to late endosomes in HeLa cells, its inhibitory effect on viral infection could in part also be attributed to trapping of virus in early endosomes which might lack components essential for uncoating. Consequently, inhibition of viral uncoating by bafilomycin cannot be taken to indicate a low pH requirement only.

Endocytosed material destined for degradation in lysosomes passes through distinct intracellular compartments. Early endosomes of tubulovesicular morphology are reached within 1 to 2 min after uptake (60). There, material en route to lysosomes is sorted from components to be recycled to the cell surface (for reviews, see references 10, 19, 38, and 40). Next, endocytic material arrives in large multivesicular perinuclear late endosomes and is finally transferred to and degraded in lysosomes. A vacuolar proton ATPase (v-ATPase) establishes an acidic pH in the lumen of endocytic organelles that gradually decreases from ca. 6.2 in early endosomes to 5.5 in late endosomes and to 4.5 in lysosomes (19, 39, 44). Two models for the basic mechanism of endocytic traffic have been proposed (24, 42). According to the maturation model, early endosomes gradually lose their ability to fuse with incoming vesicles and mature into late endosomes (14, 41, 55, 66, 67). The vesicular-shuttle model, on the other hand, predicts endosomes to be preexisting compartments communicating by shuttle vesicles (2, 18). These, also called endosomal carrier vesicles (ECV), have been shown to mediate early to late endosome transport in a microtubule-dependent fashion in BHK cells, MDCK cells, and hippocampal neurons (5, 18, 47). Recently, the budding of ECV from early endosomes has been demonstrated to depend on the activity of the endosomal proton pump in BHK cells and hence to be inhibited by bafilomycin A1 (baf), a specific v-ATPase inhibitor (3, 8). This finding has been contradicted by studies of van Weert et al. (73) in Hep-G2 cells, where baf blocked transport from late endosomes to lysosomes, without any influence on the delivery of material to late endosomes. A similar effect of baf was also observed in HEp-2 cells (72). In contrast, nocodazole blocks transport from early to late endosomes at a later stage, resulting in the accumulation of cargo in ECV. Again, this effect appears to be cell type specific, since it was observed, for example, in MDCK cells (18) but not in HEp-2 cells (71). Given these apparent discrepancies, the mechanism of transport between early and late endosomes and consequently the "endocytic transport model" might depend on the cell type.

Owing to the expression of different viral receptors, HeLa cells are widely used for the characterization of cell entry and uncoating of a number of enveloped and nonenveloped viruses (32, 33, 45, 49–52). We have previously used this system to investigate the site and the mechanism of uncoating of human rhinovirus serotype 2 (HRV2 [45, 52, 53, 62]). This nonenveloped RNA virus is a prototype of the minor receptor group of HRVs within the *Rhinovirus* genus (see, for example, reference 57). Minor-receptor-group HRVs bind to the host cell via members of the low-density-lipoprotein (LDL) receptor family (23, 34). HRV2 is internalized by receptor-mediated endocytosis and undergoes a conformational change at a pH of <5.6, thereby altering its antigenicity from "D" to "C" (26, 32, 45,

* Corresponding author. Mailing address: Department of General and Experimental Pathology, University of Vienna, Waehringer Guertel 18-20, A-1090 Vienna, Austria. Phone: 43-1-40400-5127. Fax: 43-1-40400-5130. E-mail: renate.fuchs@akh-wien.ac.at.

46). This structural modification of the viral capsid is a prerequisite for translocation of the viral RNA across the endosomal membrane and thus for successful infection. Studies with baf have revealed that the conformational change and the infection was solely dependent on the activity of the endosomal v-ATPase (52). The pH threshold of the structural modification of the viral capsid in vitro is 5.6 (20). Thus, in vivo, viral uncoating is restricted to late endocytic compartments (52). This idea is supported by the accumulation of RNA-free 80S subviral particles in isolated late endosomes by 10 min after infection. Further transport of HRV2 from late endosomes to lysosomes was monitored by lysosomal degradation of its capsid proteins that occurs 30 min after uptake (32, 45, 52).

In the past few years baf has proved to be an excellent tool for demonstrating the dependence of viral infectivity on low endosomal pH (see, for example, references 36 and 51). However, since baf might also affect transport through the endosomal system, inhibition of infection could likewise result from trapping of the virus in an endosomal subcompartment which lacks components essential for uncoating. Nocodazole does not affect endosomal pH but has been reported to inhibit endosomal transport from ECV to late endosomes. The drug might trap virus in ECV and thus allow determination of whether uncoating is only possible from later endocytic compartments. The endocytic traffic of HRV2 and fluid-phase markers in HeLa cells in the presence or absence of baf and nocodazole was therefore investigated. By using fluorescence microscopy and subcellular fractionation by free-flow electrophoresis, we show that the transport of all tracers from early to late endosomes was blocked by inhibition of endosomal acidification. Transfer from early to late endosomes depended on microtubules and required ECV. The pH in these ECV was found to be similar to the pH in late endosomes (pH $<$ 5.6). Since HRV2 infection proceeded normally in the presence of nocodazole, successful uncoating can thus take place in ECV. Taken together, baf and nocodazole can thus be applied to arrest endocytic transport processes in different subcompartments in HeLa cells.

MATERIALS AND METHODS

Chemicals. All chemicals were obtained from Sigma unless specified. baf, kindly provided by K. H. Altendorf, University of Osnabrück, Osnabrück, Germany, was dissolved in dimethyl sulfoxide (DMSO) at 20 mM and stored at −20°C. Nocodazole was dissolved in DMSO at 6 mg/ml. The final concentration of DMSO, which was also added to control samples, was kept below 1%. Fluorescein isothiocyanate (FITC)-conjugated transferrin was prepared as described previously (56). FITC-dextran (FD 70) was extensively dialyzed against Tris-buffered saline pH 7.4 and finally against phosphate-buffered saline (PBS) before use. Lysine-fixable FITC-dextran (M_r = 10 kDa), tetramethylrhodamine isothiocyanate (TMR) conjugated dextran and TMR-conjugated bovine serum albumin (TMR-BSA) were purchased from Molecular Probes (Eugene, Oreg.). FITC and TMR derivatives dissolved in PBS were diluted 1:5 in Leibowitz 15 medium (L15; Life Technologies, Vienna, Austria). Moviol 4-88 was purchased from Calbiochem and used at a concentration of 10% in aqua dest. Cy5.18-OSu (Cy5) was obtained from Amersham and coupled to dextran (M_r = 70 kDa) as described earlier (59). [^{35}S]methionine was obtained from ARC, St. Louis, Mo. Lyophilized *Staphylococcus aureus* cells (IgG-Sorb) were from The Enzyme Center, Malden, N.M. The polyclonal antibody against the cation-independent mannose-6-phosphate receptor (Man6P-R) was a kind gift of B. Hoflack (Institute Pasteur, Lilles, France).

Cell culture and virus propagation. HeLa cells (Wisconsin strain, kindly provided by R. Rueckert, University of Wisconsin) were grown in monolayers in minimal essential medium (MEM)-Eagle (GIBCO) containing heat-inactivated 10% fetal calf serum; in suspension culture Joklik's MEM (GIBCO) supplemented with 7% horse serum was used. HRV2 was propagated, labeled with [^{35}S]methionine, and purified as described earlier (65). ^{3}H-labeled poliovirus type 2 Sabin, prepared as described previously (15), was a kind gift of Peter Kronenberger.

Fluorescence microscopy. Cells were plated at low density on plastic 8-well chamber slides the day before the experiment. To investigate the effect of baf on endocytic transport of FITC-dextran (M_r = 10 kDa), cells were preincubated in serum-free L15 medium for 30 min at 37°C in the absence or presence of 20 nM or 200 nM baf; then FITC-dextran was added at 10 mg/ml, and incubation was continued for 25 min. To determine the influence of nocodazole on endocytic transport, cells were preincubated as described above, and FITC-dextran was added at 10 mg/ml for 10 min at 37°C, followed by a 15-min chase. Finally, early endosomes were labeled for 5 min with 10 mg of TMR-dextran per ml at 37°C. Where indicated, 20 μM nocodazole was present throughout preincubation and endosome labeling. Alternatively, FITC-dextran (10 mg/ml) was internalized for 10 min and chased for an additional 15 min in marker-free medium to label late endosomes. Then, TMR-dextran was added to the medium for 5 min. Thereafter, cells were cooled to 4°C and incubated without or with 20 μM nocodazole for 60 min. Finally, cells were warmed to 37°C for 5 min (with or without nocodazole). Labeled cells were cooled to 4°C, washed extensively with ice-cold PBS, fixed with 4% paraformaldehyde for 1 h at room temperature, and quenched with 50 mM NH_4Cl in PBS. Cells were mounted in Moviol and viewed with an Olympus AH2 microscope. Kodak T-Max films (3200 ASA) were used for photography.

Immunofluorescence localization of Man6P-R in cells with internalized TMR-BSA. HeLa cells were preincubated without or with 20 μM nocodazole for 30 min at 37°C. TMR-BSA (10 mg/ml) was added to the medium for 15 min, and cells were then incubated in marker-free medium (with or without nocodazole) for 10 min to label late endosomes and ECV, respectively. Subsequently, the cells were cooled, fixed with 4% paraformaldehyde for 1 h at room temperature, quenched with 50 mM NH_4Cl in PBS, washed three times with PBS (containing 1% BSA), and incubated with a rabbit antiserum against Man6P-R (1:200 in PBS containing 1% BSA and 0.005% saponin) for 20 min at room temperature. The bound antibody was detected with FITC-conjugated mouse anti-rabbit immunoglobulin G (1:50 in PBS containing 1% BSA and 0.005% saponin), and cells were mounted in Moviol as described above.

Endosome labeling for subcellular fractionation. Cells (5×10^7/ml) were preincubated for 30 min at 37°C with infection medium (MEM-Eagle containing 2% fetal calf serum [FCS] and 30 mM $MgCl_2$) in the absence or presence of the respective inhibitor (200 nM baf, 70 mM NH_4Cl, or 20 μM nocodazole). ^{35}S-labeled HRV2 (10^6 cpm) was added and internalized for 30 min at 34°C. Late endosomes were labeled by incubation of 5×10^7 cells with FITC-dextran (20 mg/ml) for 3 min at 37°C, followed by a chase of 12 min in marker-free medium. Horseradish peroxidase (HRP) was then added to a final concentration of 10 mg/ml, and cells were incubated for 3 min to label early endosomes. Alternatively, FITC-transferrin was used as an early or a recycling endosome marker, while early endosomes and late endosomes were labeled by continuous internalization of HRP. HeLa cells were washed with PBS and incubated with serum-free MEM-Eagle medium for 30 min to deplete endogenous transferrin. Cells were then allowed to internalize 20 μg of FITC-transferrin per ml for 30 min at 37°C and HRP for 25 min. Labeled cells were rapidly cooled and washed with cold PBS containing 10 mM EDTA to remove surface-bound HRV2 (31). Additionally, poliovirus that forms a stable complex with its receptor (29) was used to label plasma membranes. ^{3}H-labeled poliovirus (3×10^6 cpm) was bound to the cells in PBS for 60 min at 4°C, and unattached virus was removed by repeated washing with PBS.

Preparation of endosomes by free-flow electrophoresis. As indicated in the respective figure legends, cells labeled with virus and endocytic marker were mixed and homogenized in 4 volumes of 0.25 M sucrose in TEA buffer (10 mM triethanolamine, 10 mM acetic acid, and 1 mM EDTA, titrated with NaOH to pH 7.4) with a ball bearing homogenizer (4). Nuclei and unbroken cells were pelleted (1,000 × *g*, 10 min) to obtain the postnuclear supernatant. Microsomes were prepared by spinning the postnuclear supernatant onto a 2.5 M sucrose cushion in a TST 60.4 rotor at 100,000 × *g* for 1 h. The pellet was resuspended and adjusted to 1 mg of protein per ml in 0.25 M sucrose in TEA buffer. The sample was then subjected to gentle trypsin treatment by incubation with 3% TPCK trypsin/mg protein for 5 min at 37°C (37). The reaction was stopped by adding a tenfold excess of soybean trypsin inhibitor at 4°C. Microsomes were injected (1 ml/h) into a Bender and Hobein Elphor Vap 22 free-flow electrophoresis apparatus at 120 mA and 1,300 V with 0.25 M sucrose in TEA buffer in the chamber (37, 60, 61). A total of 92 fractions were collected (3 ml/fraction and at a rate of 3 ml/h) and assayed for protein content (6), radioactivity, fluorescence, and HRP activity.

Endosome labeling for flow cytometry. To investigate the effect of baf on endosomal pH, two different protocols were applied. In the first, HeLa suspension cells (10^8) were preincubated in 2 ml of Dulbecco MEM (DMEM) with or without baf for 30 min at 37°C. Cells were then incubated in fresh medium containing 6 mg of FITC-dextran and 1 mg of Cy5-dextran per ml with or without baf for 5 min at 37°C and chased in fresh medium with or without baf for 15 or 30 min. In the second protocol, HeLa cells were continuously labeled for 25 min with FITC-dextran and Cy5-dextran as in protocol 1; baf was then added to one aliquot, and incubation was continued in marker-free medium. For nocodazole treatment, HeLa cells (10^8) grown in suspension were pelleted and preincubated in 4 ml of suspension medium for 30 min at 37°C with or without 20 μM nocodazole. Cells were resuspended in 2 ml of DMEM containing 10% FCS with or without nocodazole. Endosomes were labeled by the addition of 6 mg of FITC-dextran and 1 mg of Cy5-dextran per ml for 5 or 15 min at 37°C, followed by incubation in marker-free medium (2 ml of DMEM containing 10% FCS) for the times indicated in the figure legends. Internalization was halted by the addition of ice-cold PBS (pH 7.4), pelleting of the cells, and washing the pellet

twice with PBS. The pellet was resuspended in PBS and analyzed immediately by flow cytometry.

Generation of pH standard curves of internalized markers by flow cytometry. Cells labeled for 5 or 15 min (see above) were pelleted and divided into eight aliquots. These were resuspended in standard pH buffers. Buffers of the desired pH (between 5.0 and 7.5) were obtained by mixing 50 mM HEPES with 50 mM morpholineethanesulfonic acid MES (both containing 50 mM NaCl, 30 mM ammonium acetate, and 40 mM sodium azide), accordingly. The samples were left on ice for 5 min for ATP depletion and for equilibration of intravesicular pH (pH clamped).

Flow cytometry. A dual-laser FACS-Calibur (Becton Dickinson Immunocytometry Systems) equipped with argon ion and red-diode lasers was used. FITC fluorescence (488-nm excitation) was determined by using a 530-nm band pass filter (30-nm band width), and Cy5 fluorescence (635-nm excitation) was determined by using a 661-nm band pass filter (16 nm band width).

Calculation of intravesicular pH. Each sample was analyzed eight times, and pH clamped samples were determined as duplicates. The mean fluorescence values of FITC-dextran and Cy5-dextran were calculated for each sample, and the autofluorescence from unlabeled samples was subtracted. The ratio of FITC to Cy5 was determined, and the intravesicular pH was calculated from the standard curve.

Immunoprecipitation of HRV2 from infected cells. Cells (5×10^5) were incubated in 500 μl of infection medium (MEM supplemented with 2% FCS and 30 mM $MgCl_2$) at 4°C with or without 20 μM nocodazole for 30 min. Cells were resuspended in fresh infection medium with or without inhibitor, incubated under slow rotation in a water bath at 34°C with 10^5 cpm of ^{35}S-labeled HRV2 for the times indicated, pelleted, and washed three times with PBS–10 mM EDTA at 4°C to remove cell-surface-bound virus. Cell pellets were lysed in 300 μl of radioimmunoprecipitation assay (RIPA) buffer (9) for 10 min at 4°C, and the cell debris was removed by centrifugation for 10 min in an Eppendorf centrifuge. Cell pellets and supernatants were processed separately for *S. aureus*-aided immunoprecipitation with monoclonal antibody 2G2 (specific for C antigen), followed by rabbit anti-HRV2 hyperimmune serum (specific for both C and D antigens) as described earlier (45). Radioactivity in the immunoprecipitates was determined by liquid scintillation counting. Alternatively, pellets were boiled in Laemmli sample buffer and analyzed on 10% polyacrylamide-sodium dodecyl sulfate (SDS) mini-gels, followed by fluorography.

Viral protein synthesis. Suspension cells (5×10^5) in 500 μl of methionine-free infection medium were preincubated for 30 min with or without baf or nocodazole and challenged with HRV2 at a multiplicity of infection (MOI) of 500 at 34°C. At 4 h postinfection, the medium was replaced with fresh methionine-free infection medium (with or without inhibitor) containing 20 μCi of [^{35}S]methionine, and incubation was continued overnight. Cells were pelleted and lysed in 300 μl of RIPA buffer, and viral proteins were immunoprecipitated with rabbit antiserum against HRV2, boiled in Laemmli sample buffer, and separated on 10% polyacrylamide-SDS minigels. Viral proteins VP1 through VP3 of the progeny virus were detected by autoradiography. Data from a single, representative experiment are shown. All experiments were repeated three times with similar results.

RESULTS

Transport from early to late endosomes in HeLa cells is dependent on low endosomal pH. First, it was verified whether baf indeed elevates the pH in endocytic compartments of HeLa cells to neutrality. Cells were incubated for 30 min at 37°C in the absence or presence of 200 nM baf, and the accumulation of acridine orange (1 μM for 10 min at 37°C) was investigated by fluorescence microscopy. In control cells, the drug accumulated in endosomes and lysosomes, which was indicative of acidic luminal pH, whereas no vesicle staining was seen in the presence of the drug; this finding demonstrates inhibition of vesicle acidification (data not shown). Alternatively, endosomes were labeled for 5 min by internalization with a pH-sensitive (FITC) and pH-insensitive (Cy5) derivative of a fluid-phase marker (dextran), and the pH of labeled compartments was calculated (for various chase times) from the ratio of the fluorescence intensities as analyzed by flow cytometry. After a 30-min chase, the average pH of labeled compartments was 6.3 in the absence and 7.4 in the presence of 200 nM baf (Fig. 1A). Thus, at this concentration, baf efficiently blocks endosome acidification. To determine the time required to dissipate endosomal pH gradients upon baf addition, endosomes were continuously labeled for 25 min with FITC and Cy5-dextran, whereupon baf was added for up to 60 min. As shown in Fig. 1B, the addition of 200 nM baf for 30 min is

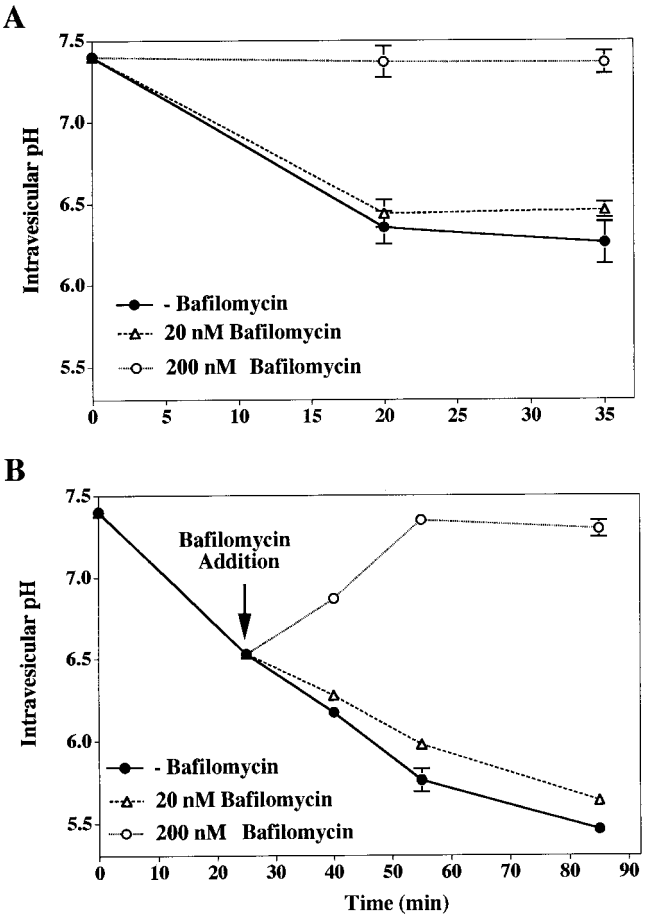

FIG. 1. baf raises the pH of early and late endosomes in HeLa cells. (A) HeLa cells were preincubated for 30 min at 37°C without or with 20 nM or 200 nM baf. They were then incubated for 5 min in medium containing 6 mg of FITC-dextran and 1 mg of Cy5-dextran per ml and subsequently chased in dextran-free medium in the absence or presence of baf. Cells were immediately cooled, washed with PBS, and analyzed by flow cytometry. (B) HeLa cells were continuously labeled with 6 mg of FITC-dextran and 1 mg Cy5-dextran per ml for 25 min. Cells were then further incubated in fresh medium without or with 20 nM or 200 nM baf (arrow). The average pH of labeled endocytic compartments was calculated with a pH calibration curve (see Materials and Methods). Times shown in both panels represent total time from the addition of FITC-dextran and Cy5-dextran. Values shown are means and standard deviations from two experiments (each sample was analyzed eight times).

sufficient to raise the average pH of all labeled compartments to neutrality. In contrast, when baf was present at a 20 nM concentration, the pH in endocytic compartments was only increased by about 0.2 pH units under either labeling condition (Fig. 1).

To investigate the influence of baf on endocytic transport in HeLa cells by fluorescence microscopy, the fluid-phase marker FITC-dextran was internalized for 25 min at 37°C in the absence or presence of 20 nM or 200 nM baf (see Materials and Methods). In control cells, vesicular accumulation of FITC-dextran resulted in a bright fluorescence staining in the perinuclear region, which is characteristic of late endosomes. When FITC-dextran was internalized in the presence of 20 nM baf, no influence on the accumulation of marker in late endosomes was observed. However, in the presence of 200 nM baf, very small peripheral vesicles were stained, resulting in a pattern typical for early endosomes (Fig. 2). To further identify the compartments accessible to endocytic markers in the presence

of baf, free-flow electrophoresis was employed to separate endosome subpopulations (60, 62). Early and late endosomes were labeled by pulse-chase with the fluid-phase markers HRP and FITC-dextran, respectively (see Materials and Methods). Furthermore, HRV2 was used as a pH-sensitive, receptor-dependent ligand (52, 53). Virus was taken up into HeLa cells for 20 min at 34°C, conditions expected to lead to accumulation in early and late endosomes. In order to demonstrate the distribution of bona fide plasma membranes (plasma membrane enzymes are also found in endosomes [37, 60]), ^{3}H-labeled poliovirus was bound to an aliquot of the cells at 4°C to label plasma membranes. The association of poliovirus with its plasma membrane receptor is stable under the conditions of free-flow electrophoresis (28). To avoid interference of fluid-phase markers and viruses, labeling of HeLa cells with the fluid-phase markers was carried out independently and cells preincubated with the various compounds were mixed before homogenization. Microsomes were prepared and subjected to FFE after gentle trypsin treatment, which is required to achieve endosome separation (37, 61). Plasma membranes labeled with ^{3}H-poliovirus were well separated from anodally shifted endosome fractions (Fig. 3A). HRP activity was mainly recovered in a slightly shifted peak representing early endosomes. The more anodally shifted peak of HRP activity reflects the arrival of the marker in late endosomal compartments already after 3 min of internalization. This finding is in agreement with a rapid transit through the early compartments (60). Although continuously internalized, the majority of HRV2 accumulated in late endosomes together with FITC-dextran. This might be due to the smaller volume of early endosomes compared to late endosomes. However, when HRV2 and fluid-phase markers had been taken up in the presence of baf, HRV2, HRP, and FITC-dextran accumulated in a compartment exhibiting the same electrophoretic mobility as the early endosomes (Fig. 3B). A similar distribution of internalized markers was observed when the vesicular pH was elevated by the presence of 70 mM NH_4Cl instead of baf (data not shown). Taken together, these results clearly demonstrate that complete inhibition of endosome acidification leads to the arrest of endocytosed ligand and fluid-phase marker in early endosomes. In the case of HRV2 this might be also due to inhibition of low-pH-dependent receptor-ligand dissociation.

Finally, the influence of different baf concentrations on HRV2 infection was determined. Cells were preincubated without or with 20 nM or 200 nM baf and then infected with HRV2. Newly synthesized viral proteins were detected by labeling of progeny virus with [^{35}S]methionine. In agreement with our previous data (62), 200 nM baf completely inhibited the infection of HeLa cells by HRV2 (Fig. 4). Although 20 nM baf failed to raise endosomal pH to neutrality and to block endocytic transport (Fig. 1 and 2), viral infection was prevented (Fig. 4). This can be explained by the pH threshold required for the conformational change of HRV2 capsid proteins that is a prerequisite for infection (45, 52). As demonstrated by Gruenberger et al. (20) maximum conversion of native virus to conformationally altered C-antigenic particles occurs below pH 5.6. Increasing the pH by 0.2 U results in a 60% inhibition of this conformational change in vitro. Thus, elevation of endosomal pH by about 0.2 U in vivo appears to be sufficient to prevent HRV2 uncoating and infection (Fig. 4).

Influence of nocodazole on endocytic transport in HeLa cells. The transfer of endocytosed material from early to late endosomes has been shown to be blocked by microtubule-depolymerizing agents (5, 18). We therefore investigated the influence of nocodazole on endocytic transport in HeLa cells. First, we confirmed the breakdown of the microtubule network

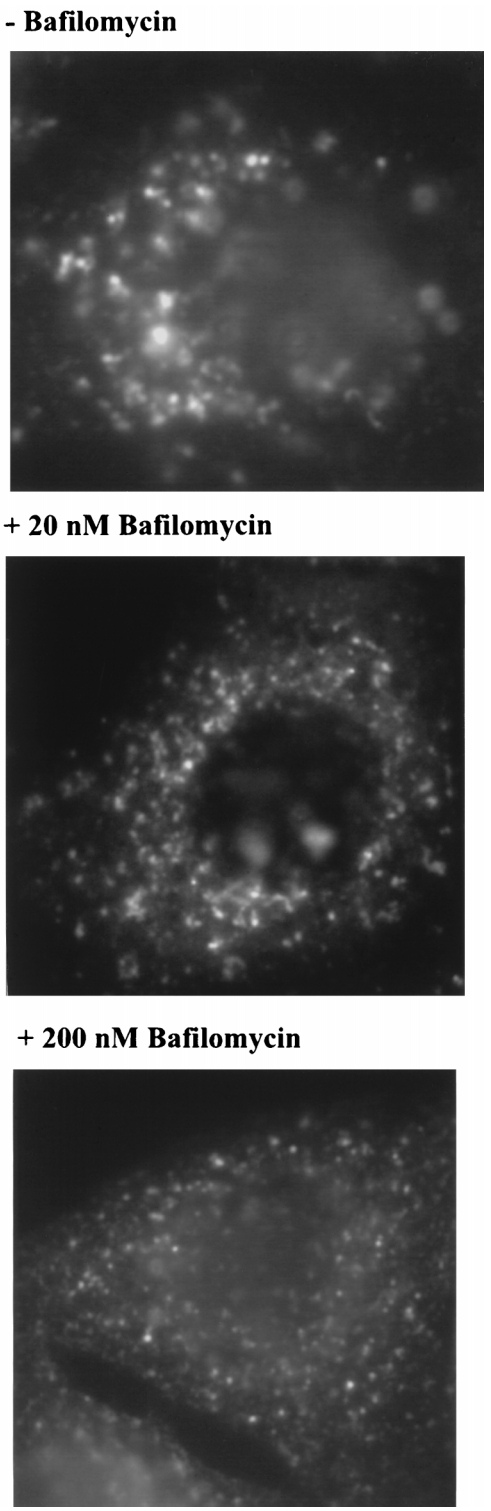

FIG. 2. Influence of baf on endocytic transport of FITC-dextran as analyzed by fluorescence microscopy. HeLa cells grown on chamber slides were preincubated without or with baf (20 nM or 200 nM) in L15 medium for 30 min at 37°C. Ten milligrams of FITC-dextran per ml was added, and endosomes were labeled for 25 min at 37°C. Cells were cooled, rinsed with PBS, fixed with 4% paraformaldehyde, quenched with 50 mM NH_4Cl in PBS, and viewed with an Olympus fluorescence microscope.

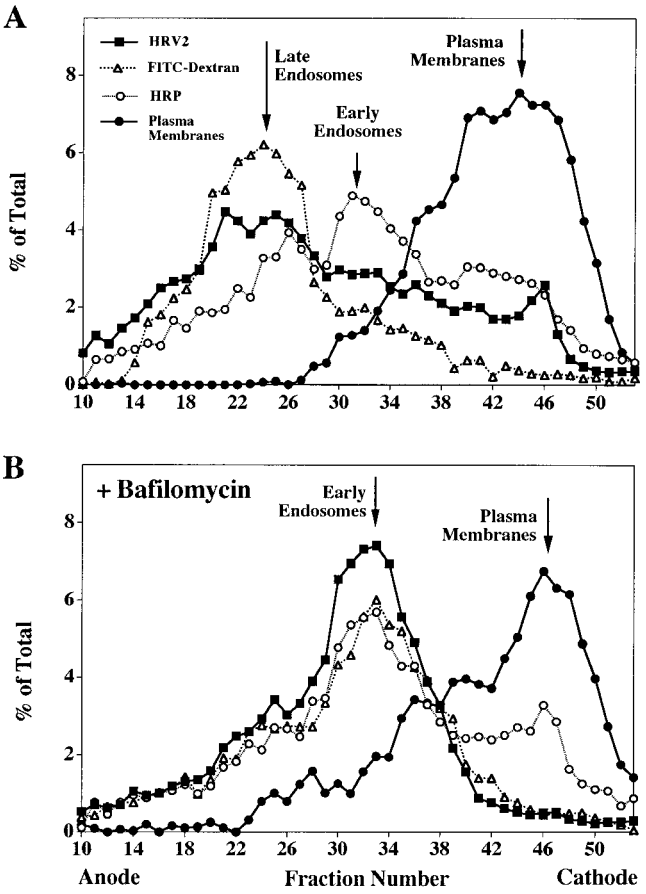

FIG. 3. baf inhibits delivery of HRV2 and fluid-phase markers to late endocytic compartments. HeLa cells preincubated without (A) or with (B) 200 nM baf (30 min, 37°C) were divided into three aliquots each. (i) Late endosomes were labeled with FITC-dextran (20 mg/ml; 3-min pulse, 12-min chase in marker-free medium); HRP (10 mg/ml) was then added for 3 min at 37°C to label the early endosomes. (ii) ^{35}S-labeled HRV2 (10^6 cpm) was internalized for 20 min at 34°C. (iii) ^{3}H-labeled poliovirus (6.5×10^5 cpm) was bound to HeLa cells for 60 min at 4°C to label plasma membranes. The aliquots of the labeled cells were cooled and combined, washed with PBS containing 10 mM EDTA to remove plasma membrane bound HRV2, and homogenized in TEA-sucrose buffer (see Materials and Methods). Microsomes were analyzed by FFE. A total of 92 fractions were collected, and protein content, radioactivity, and HRP activity, were determined. Data are expressed as the percentage of the total amount recovered after FFE.

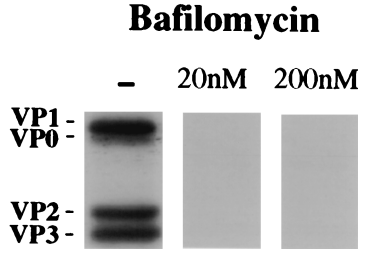

FIG. 4. baf prevents infection of HRV2. HeLa cells were preincubated in infection medium (with or without 20 or 200 nM baf) for 30 min at 34°C. HRV2 was added at an MOI of 500. At 4 h postinfection, the medium was replaced with fresh methionine-free medium containing 200 μCi of [^{35}S]methionine, and incubation was continued overnight. Cells were collected by centrifugation and lysed, and newly synthesized viral proteins were immunoprecipitated with anti-HRV2 antiserum. Viral proteins were analyzed by polyacrylamide gel electrophoresis followed by autoradiography. Where indicated, baf was present throughout the experiment.

after treatment with 20 μM nocodazole for 30 min at 37°C by indirect immunofluorescence microscopy with an FITC-labeled anti-α-tubulin antibody (data not shown). Next, the intracellular traffic of endocytic markers in the presence of nocodazole was investigated by fluorescence microscopy. FITC-dextran was chased into late endosomes, whereas TMR-dextran was internalized into early compartments. In untreated cells most of the TMR-dextran is localized in small punctate and tubular vesicles well separated from the larger, perinuclear late endosomes labeled with FITC-dextran (Fig. 5A, upper panels). Nocodazole-treated cells displayed a peripheral distribution and some colocalization of FITC-dextran and TMR-dextran (see arrowheads in Fig. 5A, lower panels). However, many compartments were accessible to FITC-dextran but not to TMR-dextran (see arrows in Fig. 5B, lower panels); these are presumed to represent ECV, which have been shown to accumulate under these conditions (18). In agreement with the results of Gruenberg and Howell (18) for BHK cells, the transport of endocytosed substances from early to late endosomes depends on the presence of intact microtubules in HeLa cells as well.

Since the distribution of late endosomes and lysosomes is also affected when microtubules are disrupted (21, 38), we verified that fluid-phase markers were indeed accumulated in ECV in the presence of nocodazole. First, late endosomes were labeled by pulse-chase with FITC-dextran, and TMR-dextran was subsequently internalized for 5 min to label the early endosomes. Cells were then cooled to 4°C, incubated for 1 h in the absence or presence of nocodazole, and subsequently warmed to 37°C for 5 min. This short incubation period was sufficient to transfer TMR-dextran from early endosomes to late endosomes in the absence of nocodazole (60, 62), resulting in colocalization of both markers in perinuclear late compartments (Fig. 5B, arrowheads in upper panels). Disruption of microtubules led to the accumulation of TMR-dextran in large vesicles (ECV) in the cell periphery. Although late endosomes labeled with FITC-dextran had acquired a random distribution in the vicinity of ECV under this condition, they are clearly distinct from ECV (Fig. 5B, lower panels). Second, the influence of nocodazole on colocalization of internalized marker with the cation-independent Man6P-R, which is primarily found in late endosomes and in the trans-Golgi network (21, 38), was investigated. For this purpose, TMR-BSA was internalized into late compartments of control or nocodazole-treated cells. Cells were then fixed and permeabilized, and localization of Man6P-R was revealed by indirect immunofluorescence. Under control conditions, considerable colocalization of endocytosed marker and Man6P-R in perinuclear compartments was seen (Fig. 5C, upper panels). However, upon internalization of the marker in the presence of nocodazole, transfer to Man6P-R-positive structures was prevented (Fig. 5C, lower panels). Again, nocodazole treatment resulted in a redistribution of the Man6P-R-labeled structures to the cell periphery. Nevertheless, the compartment where the marker is accumulated when microtubules are disrupted is clearly distinct from the late endosomes.

Luminal pH of ECV. So far, the luminal pH of those vesicles which accumulate internalized material in the presence of nocodazole (ECV) has not been determined. Therefore, kinetic analysis of endosome acidification in living cells was carried out by flow cytometry, exploiting the pH dependence of FITC-dextran fluorescence. To determine the pH of selectively labeled compartments, two protocols were applied. In the first, early endosomal compartments were labeled by a short pulse

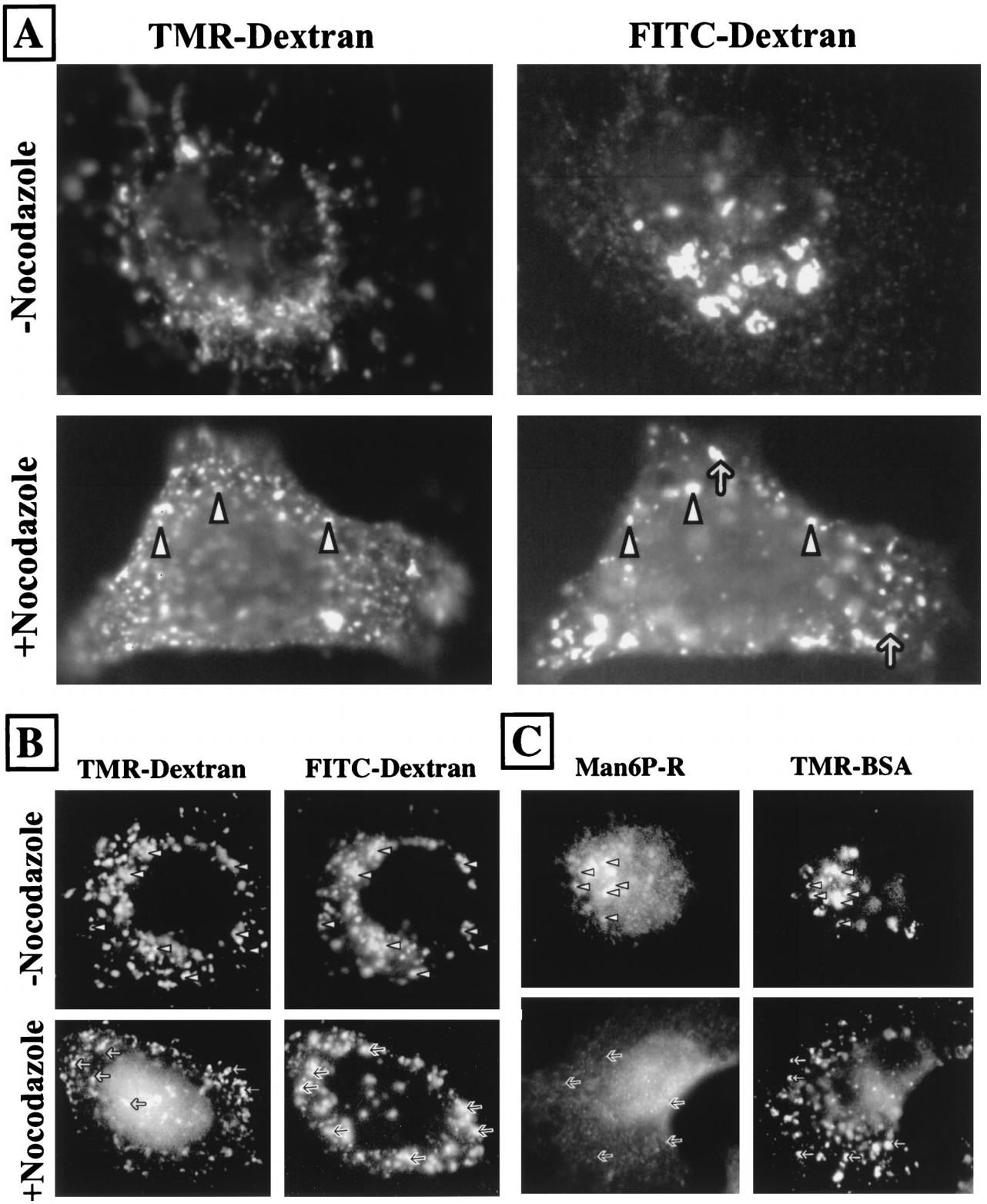

FIG. 5. Effect of nocodazole on fluid-phase marker transport in HeLa cells. (A) Cells on chamber slides were incubated without or with 20 μM nocodazole in serum-free MEM (30 min, 37°C). Late endosomes were labeled by pulse (10 min)-chase (15 min) with 10 mg of FITC-dextran per ml followed by early endosome labeling with 10 mg of TMR-dextran per ml for 5 min, and the cells were prepared for fluorescence microscopy. Where indicated, nocodazole was present throughout. FITC and TMR fluorescence images of the same cells are shown. Arrows indicate ECV; arrowheads indicate colocalization of markers in early endosomes. (B) Late endosomes were labeled by pulse (10 min)-chase (10 min) with 10 mg of FITC-dextran per ml followed by TMR-dextran (10 mg/ml) internalization for 5 min. Cells were rapidly cooled and incubated in the absence (upper panels) or presence of nocodazole for 1 h at 4°C before being warmed to 37°C for 5 min. In the absence of nocodazole, both markers colocalized in late endosomes (arrowheads, upper panels). When cells were treated with nocodazole after labeling of early and late endosomes, transfer of TMR-dextran to late, FITC-labeled endosomes (arrows, lower right panel) was arrested in EVC (arrows, lower left panel). (C) Cells were preincubated without or with nocodazole as in panel A, followed by internalization of 10 mg of TMR-BSA per ml for 15 min and a 10-min chase in marker-free medium (with or without nocodazole). Cells were cooled and fixed, and Man6P-R was detected by indirect immunofluorescence. In control cells, TMR-BSA was mainly detected in Man6P-R-positive compartments (late endosomes [arrowheads, upper panels]). Disruption of microtubules arrested the transport of TMR-BSA in ECV (arrows, lower right panel), resulting in a considerable reduction of colocalization with Man6P-R-containing structures (late endosomes [arrows, lower left panel]).

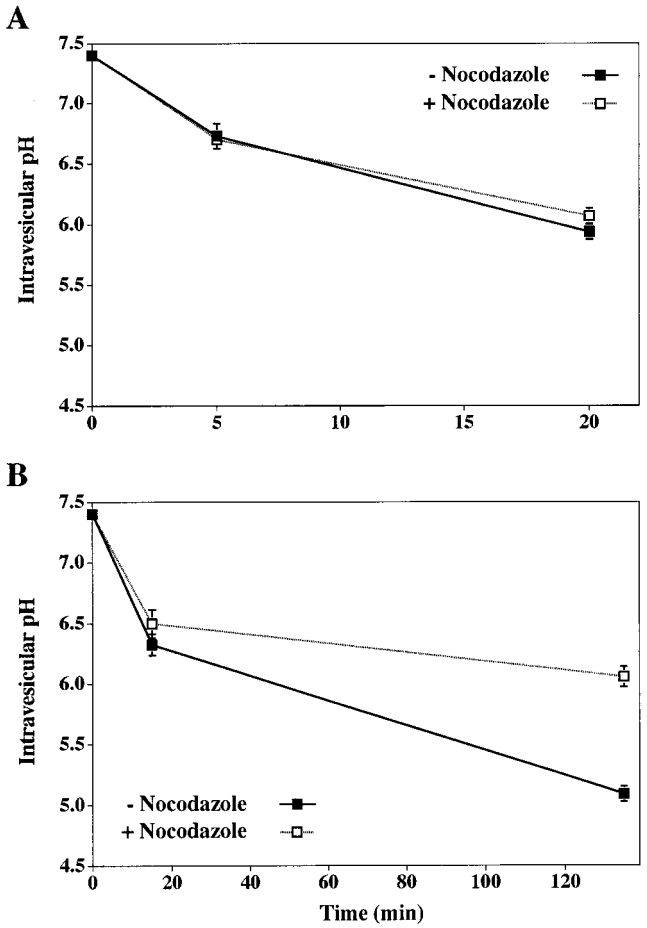

FIG. 6. Effect of nocodazole on the pH of endocytic compartments. HeLa cells were preincubated (with or without 20 μM nocodazole) in DMEM for 30 min at 37°C. (A) Endosomes were labeled with FITC (6 mg/ml)- and Cy5 (1 mg/ml)-dextran in DMEM for 5 min and then chased for 15 min in marker-free medium. (B) Cells were labeled for 15 min with FITC-dextran and Cy5-dextran (concentrations as in panel A) and chased for 120 min. The fluorescence intensity of the internalized markers was determined by flow cytometry. The average pH of endocytic compartments was calculated as described in Materials and Methods. The times shown in both panels represent the total time from the addition of FITC-dextran and Cy5-dextran. The values shown represent the means and standard deviations of two independent experiments (each analyzed eight times).

(2 min) with FITC-dextran followed by a chase in marker-free medium for 15 min. In the second, late compartments (prelysosomes and lysosomes) were labeled by a pulse for 15 min followed by a chase for 2 h. As shown in Fig. 6A, the pH of FITC-dextran-labeled compartments decreased to 6.7 within 5 min and to pH 6.0 within 20 min after internalization. Depolymerization of microtubules with nocodazole did not significantly affect the pH of the compartments reached by FITC-dextran between 5 and 20 min after internalization. Moreover, endosomes continuously labeled for 15 min (protocol 2; Fig. 6B) had a similar pH of about 6.5 regardless of the presence of the drug. When the dextran was chased into prelysosomes and lysosomes, a pH of 5.2 was found for control cells. This is in good agreement with published data (43, 55). However, in the presence of nocodazole a pH of only 6.2 was attained after a 120-min chase (Fig. 6B). This clearly demonstrates that nocodazole arrests transfer from compartments with an average pH of 6.0 to compartments of pH 5.2 (lysosomes). It should be noted that the values reported here may reflect an average for more than one type of compartment, since fluid-phase markers are expected to nonspecifically label all endocytic structures, including pH-neutral (recycling) endosomes (40, 64, 70) under the conditions applied.

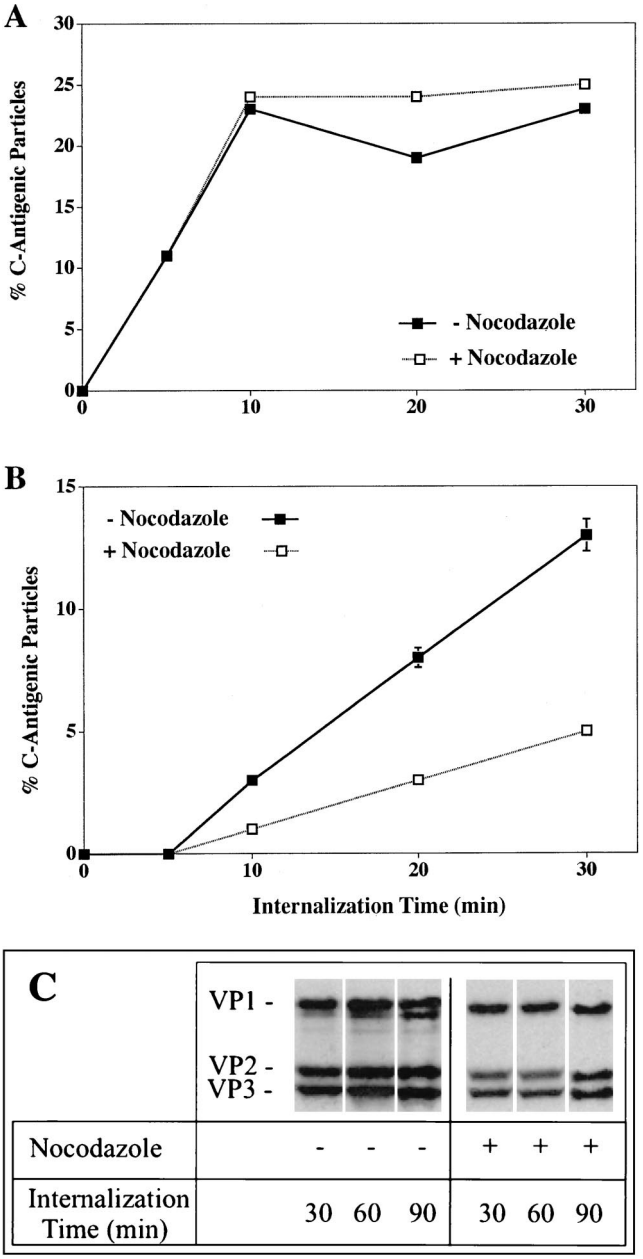

FIG. 7. HRV2 is converted to C-antigenic particles but lysosomal degradation is prevented in nocodazole-treated cells. (A and B) HeLa cells were preincubated (with or without 20 μM nocodazole) for 30 min at 34°C in infection medium and infected with [^{35}S]HRV2 (10^5 cpm) at 34°C. Aliquots were removed at 5, 10, 20, and 30 min. Samples were rapidly cooled, cells were pelleted, plasma membrane bound virus was removed with PBS–10 mM EDTA, and cell pellets were lysed in RIPA buffer. Lysates (A) and cell supernatants (B) were subjected to immunoprecipitation with monoclonal antibody 2G2, which is specific for C-antigenic particles, and polyclonal antiserum. (C) Cells were preincubated and infected as in panel A for 30 min. Unbound virus was removed with PBS, and incubation was continued with or without nocodazol for the times indicated. Virus was recovered from cell lysates by immunoprecipitation with 2G2. Viral proteins were analyzed by SDS-gel electrophoresis followed by autoradiography.

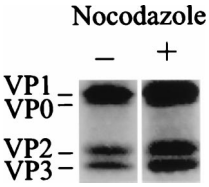

FIG. 8. HeLa cells are infected in the presence of nocodazole. Cells were preincubated in infection medium with or without 20 μM nocodazole for 30 min at 34°C. HRV2 was added at an MOI of 500. At 4 h postinfection, the medium was replaced with fresh, methionine-free medium containing 200 μCi of [^{35}S]methionine, and incubation was continued overnight. Cells were collected by centrifugation and then lysed; newly synthesized viral proteins were next immunoprecipitated with anti-HRV2 antiserum. Viral proteins were analyzed by polyacrylamide gel electrophoresis followed by autoradiography. Where indicated, nocodazole was present throughout the experiment.

To determine whether ECV can lower their luminal pH below 5.6, we took advantage of the low-pH-dependent conformational change of the HRV2 capsid that results in the formation of C-antigenic particles. Upon exposure of the virus to pH of <5.6, an epitope becomes exposed which is recognized by the monoclonal antibody 2G2 (20, 45). Consequently, the kinetics of the conformational modification of internalized [^{35}S]HRV2 was assessed in cell lysates and supernatants. C-antigenic virions were immunoprecipitated with 2G2 followed by polyclonal anti-HRV2 rabbit hyperimmune serum (to recover native virus). Radioactivity in the precipitates was then determined in a beta counter. Conversion to C antigenicity, which occurred by 5 min after uptake, was insignificantly influenced by nocodazole treatment (Fig. 7A). However, the amount of recycling of C-antigenic material to the cell supernatant was reduced by the drug (Fig. 7B). These findings imply that the pH of ECV accumulating HRV2 in the presence of nocodazole is at least 5.6. This is in agreement with results by Killisch et al. (25), who concluded from indirect data that ECV in erythroblasts are more acidic than early endosomes. For the first time, we present here direct evidence to confirm and extend these data to HeLa cells.

Further proof for inhibition of endosomal transport to lysosomes was obtained by determining the breakdown of viral proteins. The appearance of cleavage products (in particular of VP1 [20]) of HRV2 capsid proteins after 30 min of internalization at 34°C has been demonstrated to be due to lysosomal degradation, since the capsid proteins remain intact upon infection at 20°C (45). Under this condition the transfer from late endosomes to lysosomes is blocked (27). When HRV2 was internalized for 30 min and then chased for up to 90 min at 34°C, no degradation of viral proteins in the presence of nocodazole was evident (Fig. 7C); thus, transfer to late endocytic compartments (lysosomes) is clearly blocked by the drug.

HRV2 infection occurs in the presence of nocodazole. Having demonstrated that HRV2 is efficiently converted to C-antigenic particles in the presence of nocodazole, we next sought to determine whether this results in productive infection. HRV2 was internalized into HeLa cells and de novo-synthesized viral proteins were labeled with [^{35}S]methionine. As revealed in Fig. 8, viral replication occurred normally in the presence of nocodazole. Given that the transport from early to late endosomes is inhibited by the presence of the drug (Fig. 5), our data thus demonstrate productive uncoating of HRV2 from ECV.

Properties of ECV. As shown by fluorescence microscopy, fluid-phase markers accumulate in ECV in the presence of nocodazole (see Fig. 5). We thus wondered whether ECV can be separated from early and late endosomes by using FFE.

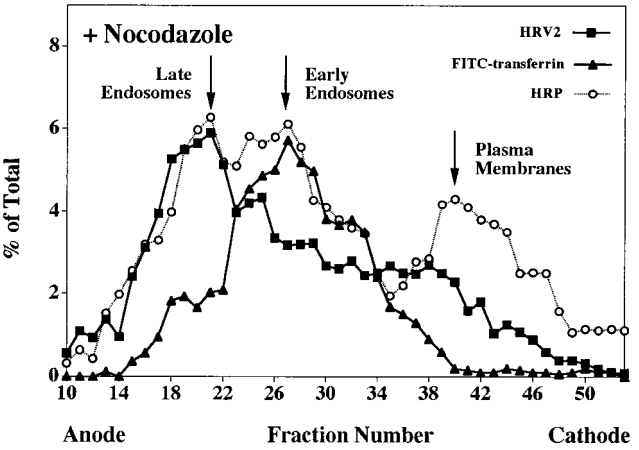

FIG. 9. ECV comigrate with late endosomes upon FFE separation. HeLa cells were preincubated in serum-free MEM with or without (Fig. 3) 20 μM nocodazole for 30 min at 37°C. Aliquots of the cell suspension were labeled with FITC-transferrin (20 μg/ml, 30 min at 37°C), HRP (10 mg/ml, 3 min, 37°C), and ^{35}S-labeled HRV2 (10^6 cpm, 30 min at 34°C), respectively. Microsomes were prepared and analyzed by FFE. Data are expressed as the percentage of the total amount of the respective marker recovered after FFE.

Early and recycling endosomes were labeled with FITC-transferrin while [^{35}S]HRV2 and HRP were continuously internalized for 20 min in the presence of nocodazole to accumulate marker in ECV. Microsomes were prepared and separated by FFE. Early and late endosomes were well separated from each other; however, the distribution of endocytic markers from control (compare with Fig. 3A) and from nocodazole-treated cells (Fig. 9) was indistinguishable. Accordingly, ECV have electrophoretic properties similar or identical to those of late endosomes and so cannot be separated by FFE. Consequently, this technique, as well as density gradient centrifugation (2), cannot be applied to ECV isolation.

DISCUSSION

Using fluorescence microscopy and subcellular fractionation techniques, we demonstrated that the v-ATPase inhibitor baf at a 200 nM concentration arrests transport of HRV2 and fluid-phase markers in early endosomes in HeLa cells. In contrast, depolymerization of microtubules with nocodazole resulted in an accumulation in ECV (which may represent either transport vesicles or early endosomes arrested during maturation to form late endosomes). Since native HRV2 was modified to its C-antigenic form in the presence of the drug, ECV must exhibit a pH of at least 5.6. Recycling of C-antigenic particles was somewhat reduced but was not prevented. ECV thus acidify their lumen to a pH almost as low as that found in late endosomes and are able to recycle their cargo to the plasma membrane (Fig. 10).

baf effects on endocytic trafficking. v-ATPases establish and maintain a low luminal pH in endocytic and exocytic compartments. These ATPases are specifically inhibited by the fungal metabolite baf. As a consequence of this inhibition, this drug has been reported to also exert secondary effects such as (i) inhibition of receptor-ligand dissociation (22), (ii) altered trafficking of transmembrane proteins (54), (iii) inhibition of budding of ECV from early endosomes (8), (iv) inhibition of late endosome-lysosome fusion (73), and (v) fragmentation of early endosomes (13). Most importantly, these secondary effects appear to vary between different cell types. We thus asked

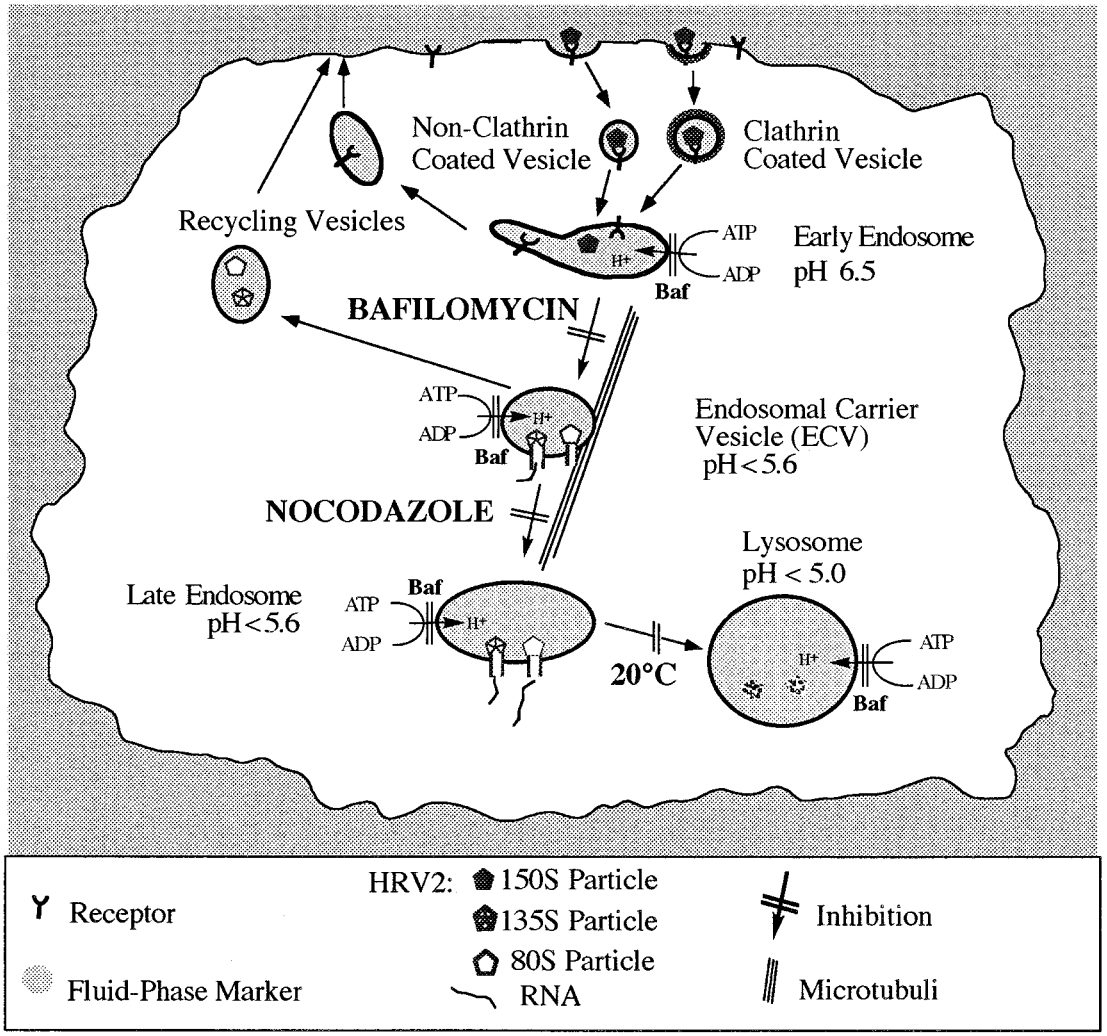

FIG. 10. Schematic representation of stages of endocytic traffic in HeLa cells blocked by baf and nocodazole. baf inhibits budding of ECV, leading to the accumulation of cargo in early endosomes, whereas nocodazol depolymerizes microtubules, thus inhibiting the transport of ECV to late endosomes, but it has only a minor effect on recycling to the plasma membrane.

whether baf also affected the endocytic route of fluid-phase markers in HeLa cells. First, the inhibition of vesicle acidification by baf was assessed. At a 200 nM concentration the drug completely inhibited vesicle acidification. However, at 20 nM the mean vesicular pH was only increased by about 0.2 pH U, and the time-dependent decrease of endosomal pH was not prevented. We then demonstrated by fluorescence microscopy that this drug indeed leads to accumulation of fluid-phase markers in very small peripheral tubular endosomes that were clearly not derived from late endosomes, since the addition of baf to FITC-dextran-loaded late endosomes did not alter their distribution. Such structures have been carefully characterized in HeLa cells under normal conditions by electron microscopy (69). It should be noted that these effects of baf were only seen at 200 nM, a concentration which elevated the pH to neutrality. Accumulation of fluid-phase marker and HRV2 in early endosomes in baf-treated cells was also shown by separation of endosome subpopulations by FFE. Although we cannot exclude with certainty that baf treatment alters the endosomal membrane composition, leading to different electrophoretic properties, the data are in accordance with the morphological studies. As far as HRV2 is concerned we cannot differentiate between the effects of baf on receptor-virus dissociation and arrest of transport. Although C-antigenic (low pH modified) HRV2 particles do not bind to the HRV2 receptors (46), the pH threshold of dissociation of HRV2 from the LDL-α_2-macroglobulin receptor family has not been determined. Nevertheless, fluid-phase markers such as dextran and HRP were also retained in early endosomes. Taken together, our results demonstrate that the transport of endocytosed macromolecules from early to late endosomes in HeLa cells depends on proper endosome acidification, regardless of whether the uptake occurs by fluid-phase or receptor-mediated endocytosis. This is in accordance with results in BHK, MDCK, and COS cells, in macrophages, and in *Dictyostelium discoideum* (3, 8, 30, 68). On the other hand, in cell lines in which maturation of early endosomes into late endosomes had been shown, baf prevented the delivery of material to lysosomes (72, 73). Recently, low-pH-dependent association of COP-I components with early endosomes was shown to be required for the formation of ECV (12, 21).

Consequences of the baf-induced transport block on viral infection. We have previously shown that baf at 200 nM completely blocks infection of HeLa cells by HRV2. Since we have proven this acid dependence in vivo and in an in vitro system in isolated endosomes (52, 53), it is legitimate to conclude that a low pH is a sine qua non condition for infection. Determination of the mean vesicular pH in HeLa cells incubated with 20 nM baf showed an increase of only 0.2 U (Fig. 1). In agreement with a pH of <5.6 required for structural modification of the viral capsid, this small pH increase was sufficient to inhibit viral infection. However, the results presented in this report call for cautious interpretation of a baf-induced block of viral infectivity since cargo remains trapped in the early endosomes in the presence of the drug, where factors required for penetration might be lacking. Entry into a late endosomal compartment could be an advantage for viruses requiring delivery to the perinuclear region for uncoating (35). Most viruses known to be uncoated along the endocytic pathway are poorly characterized with respect to the specific subcompartment where the uncoating occurs. In addition, the various effects exerted by baf in a certain cell type are usually unknown. Thus, inhibition of virus infection by baf could either be interpreted as low pH dependence and/or productive uncoating only taking place in late endocytic compartments.

Recycling to the plasma membrane in HeLa cells can occur from ECV. The subcellular localization of endocytic and exocytic compartments requires an intact and dynamic microtubular network. Consequently, microtubule depolymerization disrupts endocytic traffic at various stages, depending on the cell line under investigation (5, 71). Knowledge of the endocytic subcompartment which accumulates various markers thus allows the identification of the site of virus uncoating. We present here evidence that in HeLa cells depolymerization of microtubules by nocodazole blocks transport at the stage of ECV but only slightly inhibits recycling of modified HRV2 subviral particles (see Fig. 7). This notion is in accordance with data from Czekay et al. (11) demonstrating the recycling of megalin, a member of the LDL receptor family, from late endocytic compartments.

Proposed model of endocytic transport and endosomal pH regulation in HeLa cells. The data presented here and elsewhere (38–40, 42) suggest the following concept for endosomal pH regulation. Macromolecules internalized via endocytic coated vesicles that lack functional v-ATPases (16) are first delivered to mildly acidic early endosomes, where fast recycling of receptors (e.g., transferrin and LDL receptor) and plasma membrane proteins occurs via more-alkaline recycling endosomes (64). Budding of ECV from early endosomes leads to a pH decrease (5.6) in these compartments. Material in ECV can then either be transferred to late endosomes and further to lysosomes or be recycled to the plasma membrane. Whether these recycling compartments maintain an acidic lumen remains to be demonstrated. The maintenance of a mildly acidic pH in early endosomes depends on electrogenic interaction of the endosomal proton ATPase with Na^+/K^+-ATPase (7, 17, 58). It is thus conceivable that the budding of ECV excludes the Na^+/K^+-ATPase, which remains in the tubular portions of the early endosome and is thus recycled back to the plasma membrane. Indeed, the absence of a functional Na^+/K^+-ATPase in late endosomes has been shown. It has to be pointed out, however, that Na^+/K^+-ATPase regulates endosome acidification in some cell types (e.g., CHO [17], A549 [7], and Swiss 3T3 [74]) but not in others (e.g., K562 [63] and rat hepatocytes [1]), again demonstrating differences in endocytic membrane traffic that are dependent on cell specialization. So far, the roles of Na^+/K^+-ATPase and other factors in determining the steady-state pH of endocytic subcompartments in HeLa cells are unknown.

ACKNOWLEDGMENTS

We thank K. Altendorf and B. Hoflack for the kind gifts of baf and anti-Man6P-R antiserum, respectively.

This work was supported by Austrian Science Foundation grants P10618-MED and P12967-GEN to R.F. and P12269-MOB to D.B.

REFERENCES

1. **Anbari, M., K. V. Root, and R. W. Van Dyke.** 1994. Role of Na,K-ATPase in regulating acidification of early rat liver endocytic vesicles. Hepatology **19:** 1034–1043.
2. **Aniento, F., N. Emans, G. Griffiths, and J. Gruenberg.** 1993. Cytoplasmic dynein-dependent vesicular transport from early to late endosomes. J. Cell Biol. **123:**1373–1387.
3. **Aniento, F., F. Gu, R. G. Parton, and J. Gruenberg.** 1996. An endosomal beta COP is involved in the pH-dependent formation of transport vesicles destined for late endosomes. J. Cell Biol. **133:**29–41.
4. **Balch, W. E., and J. E. Rothman.** 1985. Characterization of protein transport between successive compartments of the Golgi apparatus: asymmetric properties of donor and acceptor activities in a cell-free system. Arch. Biochem. Biophys. **240:**413–425.
5. **Bomsel, M., R. Parton, S. A. Kuznetsov, T. A. Schroer, and J. Gruenberg.** 1990. Microtubule- and motor-dependent fusion in vitro between apical and basolateral endocytic vesicles from MDCK cells. Cell **62:**719–731.
6. **Bradford, M. M.** 1976. A rapid and sensitive method for the quantitation of microgram quantities of protein utilizing the principle of protein-dye binding. Anal. Biochem. **72:**248–254.
7. **Cain, C. C., D. M. Sipe, and R. F. Murphy.** 1989. Regulation of endocytic pH by the Na^+,K^+-ATPase in living cells. Proc. Natl. Acad. Sci. USA **86:**544–548.
8. **Clague, M. J., S. Urbe, F. Aniento, and J. Gruenberg.** 1994. Vacuolar ATPase activity is required for endosomal carrier vesicle formation. J. Biol. Chem. **269:**21–24.
9. **Collett, M. S., and R. L. Erikson.** 1978. Protein kinase activity associated with the avian sarcoma virus src gene product. Proc. Natl. Acad. Sci. USA **75:**2021–2024.
10. **Courtoy, P. J.** 1991. Dissection of endosomes, p. 103–156. *In* C. Steer and J. Hanover (ed.), Intracellular trafficking of proteins. Cambridge University Press, Cambridge, England.
11. **Czekay, R. P., R. A. Orlando, L. Woodward, M. Lundstrom, and M. G. Farquhar.** 1997. Endocytic trafficking of megalin/RAP complexes: dissociation of the complexes in late endosomes. Mol. Biol. Cell. **8:**517–532.
12. **Daro, E., D. Sheff, M. Gomez, T. Kreis, and I. Mellman.** 1997. Inhibition of endosome function in CHO cells bearing a temperature-sensitive defect in the coatomer (COPI) component ε-COP. J. Cell Biol. **139:**1747–1759.
13. **D'Arrigo, A., C. Bucci, B. H. Toh, and H. Stenmark.** 1997. Microtubules are involved in bafilomycin A1-induced tubulation and Rab5-dependent vacuolation of early endosomes. Eur. J. Cell Biol. **72:**95–103.
14. **Dunn, K. W., and F. R. Maxfield.** 1992. Delivery of ligands from sorting endosomes to late endosomes occurs by maturation of sorting endosomes. J. Cell Biol. **117:**301–310.
15. **Everaert, L., R. Vrijsen, and A. Boeye.** 1989. Eclipse products of poliovirus after cold-synchronized infection of HeLa cells. Virology **171:**76–82.
16. **Fuchs, R., A. Ellinger, M. Pavelka, I. Mellman, and H. Klapper.** 1994. Rat liver endocytic coated vesicles do not exhibit ATP-dependent acidification in vitro. Proc. Natl. Acad. Sci. USA **91:**4811–4815.
17. **Fuchs, R., S. Schmid, and I. Mellman.** 1989. A possible role for Na^+,K^+-ATPase in regulating ATP-dependent endosome acidification. Proc. Natl. Acad. Sci. USA **86:**539–543.
18. **Gruenberg, J., and K. E. Howell.** 1989. Membrane traffic in endocytosis: insights from cell-free assays. Annu. Rev. Cell Biol. **5:**453–481.
19. **Gruenberg, J., and F. R. Maxfield.** 1995. Membrane transport in the endocytic pathway. Curr. Opin. Cell Biol. **7:**552–563.
20. **Gruenberger, M., D. Pevear, G. D. Diana, E. Kuechler, and D. Blaas.** 1991. Stabilization of human rhinovirus serotype-2 against pH-induced conformational change by antiviral compounds. J. Gen. Virol. **72:**431–433.
21. **Gu, F., F. Aniento, R. G. Parton, and J. Gruenberg.** 1997. Functional dissection of COP-I subunits in the biogenesis of multivesicular endosomes. J. Cell Biol. **139:**1183–1195.
22. **Harada, M., S. Shakado, S. Sakisaka, S. Tamaki, M. Ohishi, K. Sasatomi, H. Koga, M. Sata, and K. Tanikawa.** 1997. Bafilomycin A1, a specific inhibitor of V-type H^+-ATPases, inhibits the acidification of endocytic structures and inhibits horseradish peroxidase uptake in isolated rat sinusoidal endothelial cells. Liver **17:**244–250.
23. **Hofer, F., M. Gruenberger, H. Kowalski, H. Machat, M. Huettinger, E. Kuechler, and D. Blaas.** 1994. Members of the low density lipoprotein receptor family mediate cell entry of a minor-group common cold virus. Proc. Natl. Acad. Sci. USA **91:**1839–1842.

24. **Hubbard, A. L.** 1989. Endocytosis. Curr. Opin. Cell Biol. **1:**675–683.
25. **Killisch, I., P. Steinlein, K. Romisch, R. Hollinshead, H. Beug, and G. Griffiths.** 1992. Characterization of early and late endocytic compartments of the transferrin cycle—transferrin receptor antibody blocks erythroid differentiation by trapping the receptor in the early endosome. J. Cell Sci. **103:** 211–232.
26. **Korant, B. D., K. Lonberg Holm, J. Noble, and J. T. Stasny.** 1972. Naturally occurring and artificially produced components of three rhinoviruses. Virology **48:**71–86.
27. **Kornfeld, S., and I. Mellman.** 1989. The biogenesis of lysosomes. Annu. Rev. Cell Biol. **5:**483–525.
28. **Kronenberger, P., D. Schober, E. Prchla, R. Vrijsen, O. Ofori-Anyinam, R. Vrijsen, B. Rombaut, D. Blaas, R. Fuchs, and A. Boeyé.** 1998. Uptake of poliovirus into the endosomal system of HeLa cells. Arch. Virol. **143:**1417–1424.
29. **Kronenberger, P., D. Schober, P. Prchla, D. Blaas, and R. Fuchs.** 1997. Use of free-flow electrophoresis for the analysis of cellular uptake of picornaviruses. Electrophoresis **18:**2531–2536.
30. **Lemichez, E., M. Bomsel, G. Devilliers, J. vanderSpek, J. R. Murphy, E. V. Lukianov, S. Olsnes, and P. Boquet.** 1997. Membrane translocation of diphtheria toxin fragment A exploits early to late endosome trafficking machinery. Mol. Micobiol. **23:**445–457.
31. **Lonberg-Holm, K., and J. Noble Harvey.** 1973. Comparison of in vitro and cell-mediated alteration of a human rhinovirus and its inhibition by sodium dodecyl sulfate. J. Virol. **12:**819–826.
32. **Lonberg-Holm, K., and B. D. Korant.** 1972. Early interaction of rhinoviruses with host cells. J. Virol. **9:**29–40.
33. **Madshus, I. H., S. Olsnes, and K. Sandvig.** 1984. Different pH requirements for entry of the two picornaviruses, human rhinovirus 2 and murine encephalomyocarditis virus. Virology **139:**346–357.
34. **Marlovits, T. C., T. Zechmeister, M. Gruenberger, B. Ronacher, H. Schwihla, and D. Blaas.** 1998. Recombinant soluble low-density lipoprotein receptor fragment inhibits minor group rhinovirus infection *in vitro*. FASEB J. **12:**695–703.
35. **Marsh, M., and R. Bron.** 1997. SFV infection in CHO cells: cell-type specific restrictions to productive virus entry at the cell surface. J. Cell Sci. **110:**95–103.
36. **Marsh, M., I. J. Parsons, P. Reid, and A. Pelchen Matthews.** 1993. Endocytic regulation of the T lymphocyte co-receptor proteins CD4 and CD8. Biochem. Soc. Trans. **21:**703–706.
37. **Marsh, M., S. Schmid, H. Kern, E. Harms, P. Male, I. Mellman, and A. Helenius.** 1987. Rapid analytical and preparative isolation of functional endosomes by free flow electrophoresis. J. Cell Biol. **104:**875–886.
38. **Mellman, I.** 1996. Endocytosis and molecular sorting. Annu. Rev. Cell. Dev. Biol. **12:**575–625.
39. **Mellman, I., R. Fuchs, and A. Helenius.** 1986. Acidification of the endocytic and exocytic pathways. Annu. Rev. Biochem. **55:**663–700.
40. **Mukherjee, S., R. N. Ghosh, and F. R. Maxfield.** 1997. Endocytosis. Physiol. Rev. **77:**759–803.
41. **Murphy, R. F.** 1991. Maturation models for endosome and lysosome biogenesis. Trends Cell Biol. **1:**77–82.
42. **Murphy, R. F.** 1993. Models of endosome and lysosome traffic. Adv. Cell Mol. Biol. Membr. **1:**1–7.
43. **Murphy, R. F., M. Roederer, D. M. Sipe, C. C. Cain, and R. Bowser.** 1989. Determination of the biochemical characteristics of endocytic compartments by flow cytometry and fluorometric analysis of cells and organelles, p. 221–252. *In* A. Yen (ed.), Flow cytometry: advanced research and clinical applications, vol. 2. CRC Press, Inc., Boca Raton, Fla.
44. **Murphy, R. F., S. Powers, and C. R. Cantor.** 1984. Endosome pH measured in single cells by dual fluorescence flow cytometry: rapid acidification of insulin to pH 6. J. Cell Biol. **98:**1757–1762.
45. **Neubauer, C., L. Frasel, E. Kuechler, and D. Blaas.** 1987. Mechanism of entry of human rhinovirus 2 into HeLa cells. Virology **158:**255–258.
46. **Noble, J. N., and K. Lonberg-Holm.** 1973. Interactions of components of human rhinovirus type 2 with HeLa cells. Virology **51:**270–278.
47. **Parton, R. G., C. G. Dotti, R. Bacallao, I. Kurtz, K. Simons, and K. Prydz.** 1991. pH-Induced microtubule-dependent redistribution of late endosomes in neuronal and epithelial cells. J. Cell Biol. **113:**261–274.
48. **Parton, R. G., P. Schrotz, C. Bucci, and J. Gruenberg.** 1992. Plasticity of early endosomes. J. Cell Sci. **103:**335–348.
49. **Pelchen-Matthews, A., P. Clapham, and M. Marsh.** 1995. Role of CD4 endocytosis in human immunodeficiency virus infection. J. Virol. **69:**8164–8168.
50. **Perez, L., and L. Carrasco.** 1993. Entry of poliovirus into cells does not require a low-pH step. J. Virol. **67:**4543–4548.
51. **Perez, L., and L. Carrasco.** 1994. Involvement of the vacuolar H^+-ATPase in animal virus entry. J. Gen. Virol. **75:**2595–2606.
52. **Prchla, E., E. Kuechler, D. Blaas, and R. Fuchs.** 1994. Uncoating of human rhinovirus serotype 2 from late endosomes. J. Virol. **68:**3713–3723.
53. **Prchla, E., C. Plank, E. Wagner, D. Blaas, and R. Fuchs.** 1995. Virus-mediated release of endosomal content in vitro: different behavior of adenovirus and rhinovirus serotype 2. J. Cell Biol. **131:**111–123.
54. **Presley, J. F., S. Mayor, T. E. McGraw, K. W. Dunn, and F. R. Maxfield.** 1997. Bafilomycin A1 treatment retards transferrin receptor recycling more than bulk membrane recycling. J. Biol. Chem. **272:**13929–13936.
55. **Roederer, M., R. Bowser, and R. F. Murphy.** 1987. Kinetics and temperature dependence of exposure of endocytosed material to proteolytic enzymes and low pH: evidence for a maturation model for the formation of lysosomes. J. Cell Physiol. **131:**200–209.
56. **Roff, C. F., R. Fuchs, I. Mellman, and A. R. Robbins.** 1986. Chinese hamster ovary cell mutants with temperature-sensitive defects in endocytosis. I. Loss of function on shifting to the nonpermissive temperature. J. Cell Biol. **103:** 2283–2297.
57. **Rueckert, R. R.** 1996. Picornaviridae, p. 609–654. *In* B. N. Fields and D. M. Knipe (ed.), Virology. Raven Press, New York, N.Y.
58. **Rybak, S. L., F. Lanni, and R. F. Murphy.** 1997. Theoretical considerations on the role of membrane potential in the regulation of endosomal pH. Biophys J. **73:**674–687.
59. **Rybak, S. L., and R. F. Murphy.** 1998. Primary cell cultures from murine kidney and heart differ in endosomal pH. J. Cell Physiol. **176:**216–222.
60. **Schmid, S. L., R. Fuchs, P. Male, and I. Mellman.** 1988. Two distinct subpopulations of endosomes involved in membrane recycling and transport to lysosomes. Cell **52:**73–83.
61. **Schmid, S. L., and I. Mellman.** 1988. Isolation of functionally distinct endosome subpopulations by free-flow electrophoresis. Prog. Clin. Biol. Res. **270:**35–49.
62. **Schober, D., P. Kronenberger, E. Prchla, D. Blaas, and R. Fuchs.** 1998. Major and minor-receptor group human rhinoviruses penetrate from endosomes by different mechanisms. J. Virol. **72:**1354–1364.
63. **Sipe, D. M., A. Jesurum, and R. F. Murphy.** 1991. Absence of Na^+,K^+-ATPase regulation of endosomal acidification in K562 erythroleukemia cells—analysis via inhibition of transferrin recycling by low temperatures. J. Biol. Chem. **266:**3469–3474.
64. **Sipe, D. M., and R. F. Murphy.** 1987. High-resolution kinetics of transferrin acidification in BALB/c 3T3 cells: exposure to pH 6 followed by temperature-sensitive alkalinization during recycling. Proc. Natl. Acad. Sci. USA **84:**7119–7123.
65. **Skern, T., W. Sommergruber, D. Blaas, C. Pieler, and E. Kuechler.** 1984. Relationship of human rhinovirus strain 2 and poliovirus as indicated by comparison of the polymerase gene regions. Virology **136:**125–132.
66. **Stoorvogel, W.** 1993. Arguments in favour of endosome maturation. Biochem. Soc. Trans. **21:**711–715.
67. **Stoorvogel, W., G. J. Strous, H. J. Geuze, V. Oorschot, and A. L. Schwartz.** 1991. Late endosomes derive from early endosomes by maturation. Cell **65:**417–427.
68. **Temesvari, L. A., J. M. Bush, M. D. Peterson, K. D. Novak, M. A. Titus, and J. A. Cardelli.** 1996. Examination of the endosomal and lysosomal pathways in *Dictyostelium discoideum* myosin I mutants. J. Cell Sci. **109:**663–673.
69. **Tooze, J., and M. Hollinshead.** 1991. Tubular early endosomal networks in AtT20 and other cells. J. Cell Biol. **115:**635–653.
70. **van der Sluijs, P., M. Hull, P. Webster, P. Male, B. Goud, and I. Mellman.** 1992. The small GTP-binding protein rab4 controls an early sorting event on the endocytic pathway. Cell **70:**729–740.
71. **van Deurs, B., P. K. Holm, L. Kayser, and K. Sandvig.** 1995. Delivery to lysosomes in the human carcinoma cell line HEp-2 involves an actin filament-facilitated fusion between mature endosomes and preexisting lysosomes. Eur. J. Cell Biol. **66:**309–323.
72. **van Deurs, B., P. K. Holm, and K. Sandvig.** 1996. Inhibition of the vacuolar H^+-ATPase with bafilomycin reduces delivery of internalized molecules from mature multivesicular endosomes to lysosomes in HEp-2 cells. Eur. J. Cell Biol. **69:**343–350.
73. **van Weert, A. W., K. W. Dunn, H. J. Gueze, F. R. Maxfield, and W. Stoorvogel.** 1995. Transport from late endosomes to lysosomes, but not sorting of integral membrane proteins in endosomes, depends on the vacuolar proton pump. J. Cell Biol. **130:**821–834.
74. **Zen, K., J. Biwersi, N. Periasamy, and A. S. Verkman.** 1992. Second messengers regulate endosomal acidification in Swiss 3T3 fibroblasts. J. Cell Biol. **119:**99–110.